

Systematic Generalization for Predictive Control in Multivariate Time Series

Hritik Bansal*

Electrical Engineering
IIT Delhi
New Delhi, India
hbansal10n@gmail.com

Gantavya Bhatt*

Electrical and Computer Engineering
University of Washington
Seattle, USA
gbhatt2@u.washington.edu

Pankaj Malhotra

TCS Research
New Delhi, India
malhotra.pankaj@tcs.com

Prathosh A.P.

Electrical Engineering
IIT Delhi
New Delhi, India
prathoshap@iitd.ac.in

Abstract—Prior work has focused on evaluating the ability of neural networks to reason about novel combinations from known components, an intrinsic property of human cognition. In this work, we aim to study systematic generalization in predicting future state trajectories of a dynamical system, conditioned on past states’ trajectory (dependent variables), past and future actions (control variables). In our context, systematic generalization implies that a good model should perform well on all new combinations of future actions after being trained on all of them, but only on a limited set of their combinations. For models to generalize out-of-distribution to unseen action combinations, they should reason about the states and their dependency relation with the applied actions. We conduct a rigorous study of useful inductive biases that learn to predict the trajectories up to large horizons well, and capture true dependency relations between the states and the controls through our synthetic setup, and simulated data from electric motors.

Index Terms—Systematic generalization, Multivariate time series, States and Controls, Forecasting.

I. INTRODUCTION

The ability to learn the forward predictive model of state trajectories conditioned on past states, past actions, and future action trajectories is an important contribution of the deep learning revolution. The ability to learn such predictive models is leveraged in a wide variety of scenarios where the constituent objects behave in a highly complex fashion as a consequence of applied actions [1], [15], [26].

Additionally, there has been a lot of attention towards assessing the limitations of neural networks and understanding the extent to which they can generalize to novel scenarios that do not occur in the training distribution. Systematic generalization forms an essential part of such studies, and its roots in the study of human cognition [17], [18]. Being able to show systematicity implies that the models can compose the learned knowledge derived from training data in a meaningful way in new settings, e.g., the ability to understand “walk left” after training on “right”, “walk left” and “run right”. In our context of multivariate time series, where the state trajectories change as a consequence of applied actions, *a good model should be able to reason about all possible combinations of future controls (actions) despite being trained on a subset of them.*

This paper analyzes a fundamental question: what are the key architectural inductive biases that achieve better generalization than generic models? An idea that comes to mind is to construct the models to replicate the underlying structure of the data closely and learn the correct dependency relations from the data. This is the hypothesis we set to evaluate here for the models trained to predict the future state trajectories conditioned on the past states, past controls, and planned future control by treating these time series as temporal segments III. We do not beat the state-of-the-art models on time series forecasting but rather present a useful line of work on understanding which architectural choices are more likely to generalize better IV.

We analyze our approach on broadly two experimental setups – synthetic setup of non-linear autoregressive moving average (NARMA) time series VI-A and simulated data from electric motor VI-B. These experiments highlight the quality of the learned transition model (the model that maps the conditioning random variables to the future random variable) in terms of their predictive prowess to unseen action combinations while capturing real underlying dependency relations between the states and the control inputs.

II. RELATED WORK

Systematic Generalization: Systematic generalization has recently gained a lot of traction due to its ability to uncover neural networks’ compositional capabilities. The work by [4], [6] suggests that sequence-to-sequence models test poorly on the data points that require compositional skills and latch onto data-specific regularities. The work on visual question answering models by [5] corroborates the negative generalization capabilities of generic models and highlights that systematicity can be improved by adding explicit structure to deep learning models. Similarly, [7] study systematic generalization with Transformer-based models. Despite being a ubiquitous concept in the domain of natural language, we aim to extend it to the neural networks used for time-series modeling in this paper.

Time Series Forecasting: There have been various models such as autoregressive models and state-space models used for time series forecasting that require domain-specific rules to be known or require assumptions made regarding the property of the time series [8]. With the advent of deep learning,

* Equal Contribution

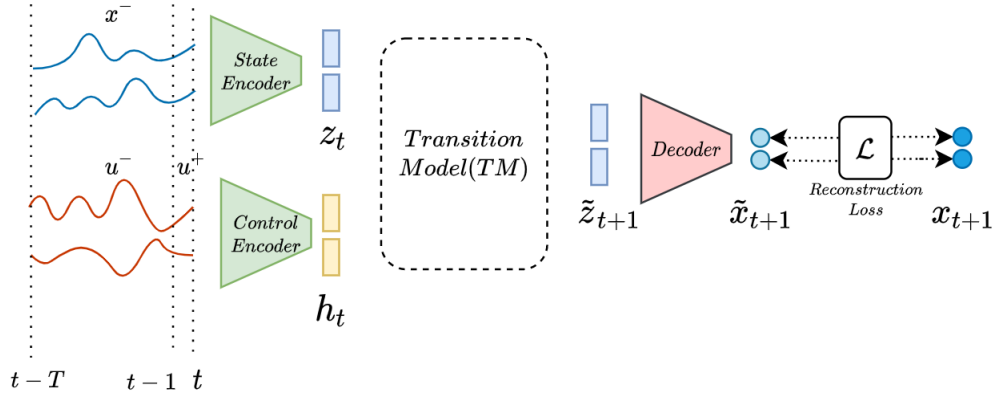


Fig. 1: The pipeline of our architecture for 1 step prediction. Temporal segments of state and control variables are first encoded, then passed through a transition model (MLP/Structured) and then the future states are evaluated using a linear decoder.

various neural network architectures have been successfully able to forecast in highly non-linear time series spaces [9], [10], [12], [23]. In this work, we ask a finer question: what key architectural choices enable systematic generalization and capture some level of underlying interactions between the states and the controls?

Representation Learning: The ability to learn high-level representations from the data with neural networks in an end-to-end fashion is also a very popular idea [11]. Recent work proposes different methods to learn useful representations of the time series data in an unsupervised way that can be leveraged to perform well on downstream tasks such as classification [2], [3]. These methods choose to have an additional contrastive loss term, which has shown to be useful for representation learning across various applications [13], [14], [26]. However, in this paper, we purely evaluate the models’ systematic generalization capabilities with different architectural inductive biases and leave the deployment of additional loss terms to improve systematicity as future work.

Action-Conditioned State Trajectory Prediction: The problem of learning dynamics of a system to predict state trajectories conditioned on the applied control input (action) is a primary focus of robotics and reinforcement learning [15]. [1] presented an approach to learning the distribution over future state trajectories conditioned on past states, a past action, and future actions using variational autoencoder. However, our formulation does not consider stochasticity in environment transitions or observations, hence limited to deterministic dynamics world models. The models need to reason computationally in terms of states, controls, and their dependencies for them to predict future dynamics of multiple states well [26]. Our work analyzes the effect of strong inductive biases in the latent transition models to predict future state trajectories.

III. SEGMENT BASED DYNAMICS MODEL

Similar to [1], we consider a dynamical system with \mathbf{x}_t as states and \mathbf{u}_t as the control input. Our goal is to efficiently

learn the future dynamics of this system, which robustly predicts over the long horizons even in the presence of sensory noise and delays in the control input. To learn dynamics, often one-step models of dynamics are considered, which take current state \mathbf{x}_t and control input \mathbf{u}_t , to predict \mathbf{x}_{t+1} . However, when such a method is used in tandem for multiple time steps, the predicted trajectory diverges from the actual trajectory.

Therefore, instead of just using the current state \mathbf{x}_t , we consider T previous inputs in addition to the current states: $x^- = \{\mathbf{x}_{t-T}, \dots, \mathbf{x}_{t-1}, \mathbf{x}_t\}$ and similarly previous and current inputs: $u^- = \{\mathbf{u}_{t-T}, \dots, \mathbf{u}_{t-1}\}$, $u^+ = \{\mathbf{u}_t\}$, to predict the future state \mathbf{x}_{t+1} . Including a temporal segment of previous control inputs also helps in the situation when the system has a delay in the control inputs. In this paper, we consider the dimension of state \mathbf{x} to be equal to that of the control \mathbf{u} .

IV. ARCHITECTURE

Our framework consists of 3 stages: state and control encoders, a transition model, and a linear decoder (Figure 1). To explain our pipeline, we consider a dynamical system with 2 state variables and 2 control variables.

A. State and Control Encoder

In our framework, we have separate encoders for the state and the control time series. Each encoder comprises a 1D causal convolutional neural network (causal-CNN). Causal convolutions map a sequence to a sequence of the same length such that the i^{th} output sequence is calculated using the values up till i^{th} element of the input [2]. Each dimension of the state variable contributes to one channel of the input to the CNN i.e., if x is two-dimensional, the input to the CNN would have two channels. However, we consider two variants of encoding possibilities for the control variables. First, **common control** encoder where each dimension of the control variable contributes to one channel of the input to the CNN, identical to the state encoder. Second, **separate control (SC)** encoder where we have a separate causal CNN with one output channel for each control input time series. Separate control encoders

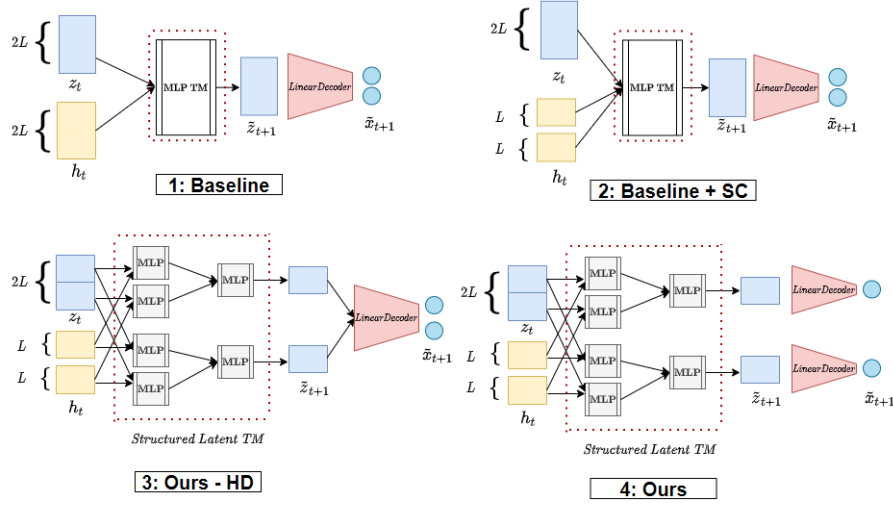


Fig. 2: Transition Models and Decoders. In model 1 and 2, we use MLP as a transition model, while in the model 3 and 4, we use a structured latent model which helps in systematic generalization.

do not share weights. In the later choice of encoding, we have used the fact that control inputs are exogenous variables and deserve the independent treatment of their own. We posit that having a common CNN encoder for the control variables learns spurious correlations between the controls. The number of output channels for the state encoder and common control encoder is kept to be equal to the dimension of the control variable.

For the cases where the length of a temporal segment (T) is very long, we can demarcate each that temporal segment into smaller segments (K segments each of length T/K) and use causal CNN over these shorter segments of length T/K . Final embedding for the complete segment is obtained using a recurrent neural network (such as LSTM) [3].

B. Transition Model and Decoder

After passing the state and control temporal segment through their respective encoders, we get their representations \mathbf{z}_t and \mathbf{h}_t , respectively. Let the dimension of these representations for each state and control variable be L . Thus, a scenario of 2 state variables and 2 control variables would yield \mathbf{z}_t and \mathbf{h}_t to be of $2L$ dimension each. Consider the architectures 1-4 in Figure 2. In Architecture 1, we have a common control encoder, while in the others, we have a separate control encoder. We indicate this by displaying \mathbf{h}_t for each input separately. We implement a transition model which takes these \mathbf{z}_t and \mathbf{h}_t , and predicts the representation for future state, $\tilde{\mathbf{z}}_{t+1}$. To test different inductive biases, we consider two major variants of the transition model.

1) *MLP Transition Model*: The MLP transition model concatenates the representations \mathbf{z}_t and \mathbf{h}_t . The concatenation operation is represented as two incoming arrows in Figure 2. Following the concatenation, the transition model passes them through a 2-layer MLP, producing a vector $\tilde{\mathbf{z}}_{t+1}$ of dimension $2L$. In Figure 2, this transition model is presented as the

Baseline model as it lacks any structural inductive bias. **Baseline + SC** is identical to baseline, except it contains control embeddings coming from separate causal CNN encoders.

2) *Structured Latent Space Transition Model*: In this case, we intend to have a useful inductive bias in form of factored representation space that is less prone to learning spurious correlations as it structurally resembles the kind of rules it is supposed to learn from the data. A good transition model is necessary to forecast well and improve performance on other downstream tasks. We empirically verify the usefulness of such inductive bias in the Section VI.

The structured latent space allows for a systematic exchange of information between the state and control inputs, as shown in the Figure 2. Let us assume a scenario where we have n state and n control variables. Hence, the state encoder and control encoder output n state representations, $z_t(i)$, and n control representations, $h_t(i)$, respectively, such that the dimension of $h_t(i)$ and $z_t(i)$ is L .

Firstly, we get $E_t^j = \{e_t^{ij}, i \in \{1, 2, \dots, n\}\}$, for every n state and control variable as:

$$e_t^{ij} = f_1^{ij}([z_t(i); h_t(i)]) \quad \forall j \in 1, 2, \dots, n \quad (1)$$

where $;$ represents the concatenation operator, f_1^{ij} represents a 1-layer MLP which maps the input of dimension $2L$ to a output of dimension L . Here, e_t^{ij} captures the dependencies between the state and control representations to predict the trajectory of state x_{t+1}^j . We collate all such dependency relations, and pass them through another 1-layer MLP, f_2^j to get the predicted representation of the future states:

$$\tilde{z}_{t+1}(j) = f_2^j([e_t^{1j}; e_t^{2j}; \dots; e_t^{nj}]) \quad \forall j \in 1, 2, \dots, n \quad (2)$$

Thus, f_2^{ij} takes the input of nL dimension to output dimension of L . Figure 2 presents this architecture as **Ours**. All of f_1^{ij} and f_2^{ij} correspond to a different neural network.

3) *Decoder*: After we get $\tilde{\mathbf{z}}_{t+1} = [\tilde{z}_{t+1}^1; \tilde{z}_{t+1}^2; \dots; \tilde{z}_{t+1}^n]$ from the transition model, we pass it through a decoder, to obtain the predicted next states, $\tilde{\mathbf{x}}_{t+1}$. Based on the way we decode, we construct two possibilities. Firstly, we have **common decoding**, where we directly pass nL dimensional $\tilde{\mathbf{z}}_{t+1}$ through decoder to generate a n dimensional $\tilde{\mathbf{x}}_{t+1}$. Here, reconstruction loss is calculated between the predicted states ($\tilde{\mathbf{x}}_{t+1}$) and the ground truth trajectory (\mathbf{x}_{t+1}). This loss gets back-propagated through the complete pipeline, and trains it end-to-end. This decoding scheme is applicable for both the MLP transition model and the structured latent transition model. On the other hand, we define a **hard decoder (HD)**, where we pass the representation for each predicted state variable $\tilde{z}_{t+1}(j)$ from structured latent transition model to separate decoders. Across all the settings, the decoder is implemented using 1 fully connected network¹. This model is presented as **Ours - HD** in Figure 2.

C. Multi-step Prediction

In our framework, we train the models for multi-step prediction. In the previous section and Figure 1, we have described the pipeline for one-step prediction. For multi-step predictions, the transition model predicts future state representations (\tilde{z}_{t+1}) from z_t and h_t . Thus, to get the representations \tilde{z}_{t+M} , we need to unroll the transition model and provide h_t to h_{t+M-1} , while we will recursively use the predicted state representations as input to the transition model. We did not use the predicted states, x_{t+1} to predict future state representations, z_{t+2} as periodically jumping back to the true path will generate artifacts in the learned trajectories [24].

V. TRAINING SETTINGS

Throughout our experiments, the temporal segment’s length does not require the use of a recurrent network. To compute the loss function, we train our network in a multi-step prediction to evaluate the reconstruction loss on the next five prediction steps. All the models are trained for ten different random seed initializations with ADAM optimizer [19]. We consider four versions of the architecture, based on the type of control encoder- common control v/s separate control, type of transition model- MLP v/s structured latent transition model, and decoder choice common v/s hard decoding. We write separate control as SC and hard decoding (or separate decoding) as HD. Other training settings and the choice of hyperparameters are available at our codebase.²

VI. EXPERIMENTS

Our goal of this experimental section is to study the effect of various inductive biases on their ability to 1) learn a good transition model in the latent space that helps in 2) accurate forecasting up to large horizons, and 3) generalizes

systematically to an unseen combination of future actions (control variables).

A. Synthetic Data

We obtain multivariate time series using Non-Linear Autoregressive Moving Average (NARMA) [20] generators from TimeSynth Library [21]. For our purpose, we use the following modified dynamical equation of NARMA signals:

$$x_{i,t+1} = a_i x_{i,t} + b_i x_{i,t} \sum_{k=t-m}^t x_{i,k} + \sum_{j=1}^n c_{i,j} u_{j,t} u_{j,t-m} + d_i \quad (3)$$

where x_i is the state (dependent or endogenous) variable in the i^{th} dimension, u_j is the control (exogenous) variable in the j^{th} dimension, n equals the dimension of the state and control variable in our framework ($1 \leq i \leq n, 1 \leq j \leq n$), m is the order of non-linear interactions, t is the current timestamp, $c_{i,j}$ controls the interaction between the control u_j and the state x_i (VI-A1), and a_i, b_i, d_i are parameters specific to state x_i . In our experiments, we fix $n = 2$ which makes it easy to manipulate different state and control variable relations, and have fixed $m = 10$ for our experiments.

We deliberately introduce spurious correlations between the two ($n = 2$) controls using:

$$u_{2,t} = \alpha u_{1,t} + (1 - \alpha)k \quad \forall t \quad (4)$$

where $k \sim U(0, 1)$, $u_{1,t} \sim U(0, 1)$, and $\alpha \sim U(p, q)$. Here α acts as a correlation factor between the two control variables, tweaking which allows us to test generalization to unseen future control combinations (VI-A2).

1) *NARMA Scenarios*: From Equation 3, it is clear that $c_{i,j}$ determines the causal relations between the states and the controls across dimensions e.g., $c_{1,2} = 0$ and $c_{2,1} \neq 0$ implies that u_2 does not effect x_1 but u_1 effects x_2 . Following the same principle, we create four NARMA scenarios in our work (Figure 3). These scenarios allow us to assess which dependency relations are better modelled by the learned latent transition model.

Scenario 2 differs from Scenario 3 by the strength of causal relation between the controls and states governed by parameter $c_{i,j}$. We keep $(c_{1,1}, c_{1,2}, c_{2,1}, c_{2,2}) = (1.5, 0, 0.5, 0.55)$ for Scenario 2, and $(c_{1,1}, c_{1,2}, c_{2,1}, c_{2,2}) = (1.5, 0.15, 0, 0.55)$ for Scenario 3. Among all the four scenarios considered, Scenario 1 is the most challenging one as the models cannot predict the future trajectory of its states without learning the underlying interactions perfectly. It is important for the models to capture the true underlying dependencies to forecast well up to large horizons.

2) *Systematic Generalization Setup*: In addition to performing well on control combinations, (u_1, u_2) , that have been observed in the training phase, a robust model should be able to reason about unseen combinations of future controls after being trained on all of them i.e., observing all individual values of u_1 and u_2 . Figure 4 shows the joint distribution of control inputs (u_1, u_2) .

¹In case when we have a mismatch in the number of states and control input, we will use a 1D CNN decoder, with the number of input channels being the number of control variables and the number of output channels being the number of state variables. However in this case we only have a common decoder.

²https://github.com/Hritikbansal/MultivariateTimeSeries_Generalization

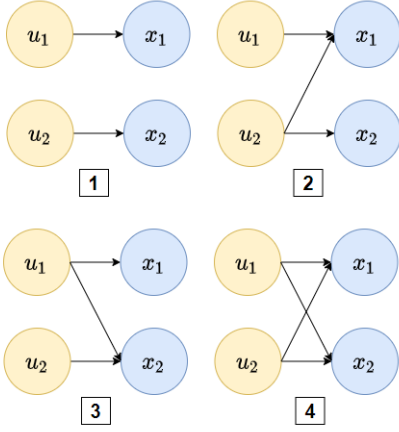


Fig. 3: We consider four scenarios in our synthetic dataset. Out of the four scenarios, it is most difficult to learn correct dependencies in the first one, which we show using out of distribution testing examples.

We test systematic generalization by restricting the combination of controls seen during training by choosing $\alpha \sim U(0.4, 0.7)$ in Equation 4 (Orange region in Figure 4). For out-of-distribution (OOD) testing, we generate controls by choosing $\alpha \sim U(0, 1)$. We ensure that the future controls lie outside the region seen by the models during the training (Blue region in Figure 4). All control inputs follow the identical setup across four scenarios described in VI-A1.

3) *Results:* We set up quantitative experiments for evaluating the quality of the learned transition model (VI-A3a), and the quality of state-control interactions captured by the models (VI-A3b).

We train our models on 8k temporal segments over states and controls and test them on 2k segments. We fix the length of a segment $T = 11$ and train the models using multistep prediction (5-time steps) in the future. Thus, five reconstruction losses are added to give the total loss, which gets back-propagated to make a single update to the whole pipeline. Multistep prediction during training helps avoid learning sub-optimal transition models that could perform well on a single time step but may perform worse on larger horizons [24]. We use Mean-Squared Error (MSE) to evaluate the quality of future predictions (forecasting) across different NARMA scenarios. We average report MSE across ten different random seeds for all the models in consideration.

a) *Forecasting – IID vs OOD Performance:* We provide results for the proposed model and the baseline in Table I. The MSE values are reported for single-step prediction during testing. Each row corresponds to a scenario from VI-A1. We divide the results into three attributes: forecasting MSE when the future controls are sampled from the same joint distribution as observed during the training phase (MSE IID), forecasting MSE when future controls lie outside observed

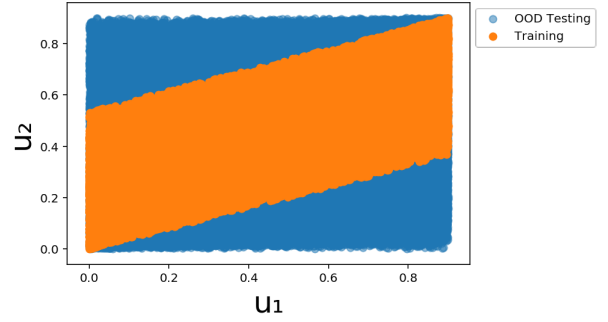


Fig. 4: Distribution of control inputs. During the training, we expose the models with the control inputs in the orange region. At the test time, we evaluate for the inputs in the blue region (the upper and lower triangles)

joint distribution of future controls (MSE OOD), and relative error between MSE IID and MSE OOD.

From Table I, it can be concluded that the baseline, the model without any factored representations in the latent transition model and without separate treatment to control encoders, performs worse (10x) on OOD testing across all scenarios. For the first three scenarios, this simplest architecture performed as well as the other architectures on the MSE IID metric. This confirms our evaluation procedure’s robustness, as the model without appropriate inductive bias performs worse on MSE OOD and relative error metric. The MSE values are towards a higher end for all the models in scenario four as it possesses highly non-linear complex dynamics due to its dependency relations.

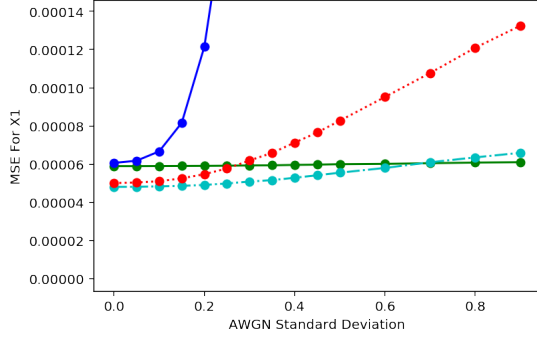
The results also highlight the usefulness of the proposed factored latent transition model (**Ours**). In scenarios 1-3, the models need to prune the non-existent dependencies and avoid capturing false interactions for good forecasting performance. In 2 of these 3 scenarios, the models with structural transition model (**Ours**, **Ours - HD**) gave the least relative error. Additionally, it is interesting to see that the separate treatment of controls also improves the performance in the absence of a structural transition model. This indicates that having separate encoders for independent control variables guides the learning towards a better transition model.

b) *Intervention Testing:* By now, we have established that useful inductive biases help to generalize to unseen combinations through quantitative forecasting errors. However, it is not clear if the models are learning the correct relations between the states and the controls for future predictions. To answer this question, we subject our models to intervention testing. From the theory of causality, [25], if a variable X is not a cause of variable Y , then external intervention on X should not affect the values of Y , i.e., changing X should not change Y . As we already know the true causal relations in our NARMA scenarios (Figure 3), we leverage intervention testing to assess what is being learned by the models.

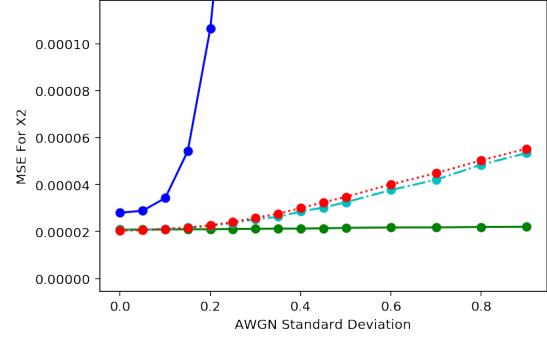
In scenario 1, changing the value of future control u_2^+ , using additive white gaussian noise (AWGN), should not change the

NARMA Scenario	MSE IID ($\times 10^{-5}$)				MSE OOD ($\times 10^{-5}$)				(OOD-IID)/IID			
	Baseline	Baseline+SC	Ours-HD	Ours	Baseline	Baseline+SC	Ours-HD	Ours	Baseline	Baseline+SC	Ours-HD	Ours
1	0.89	0.71	0.69	0.80	27	3.18	2.75	2.74	29.24	3.52	3	2.43
2	1.30	1.02	1.08	1.33	31	3.82	4.67	5.29	22.71	2.73	3.34	2.97
3	1.46	1.06	0.94	1.00	23	3.53	3.08	3.50	14.86	2.35	2.29	2.5
4	5.53	1.31	1.24	1.42	160	4.45	5.12	5.10	27.23	2.38	3.13	2.58

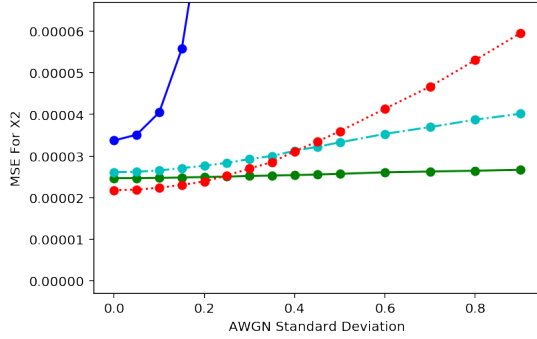
TABLE I: Results on a synthetic dataset. Note that models with structured latent TM outperform the ones without MLP TM.



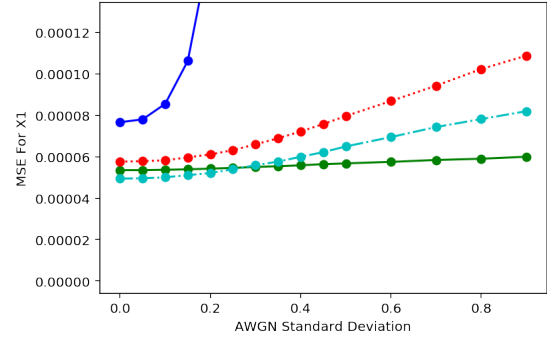
(a) MSE of x_1 on perturbing u_2 with additive gaussian noise of given standard deviation.



(b) MSE of x_2 on perturbing u_1 with additive gaussian noise of given standard deviation.



(c) MSE of x_2 on perturbing u_1 with additive gaussian noise of given standard deviation.



(d) MSE of x_1 on perturbing u_2 with additive gaussian noise of given standard deviation.

Fig. 5: Variation of MSE of the state variable, when adding white Gaussian noise on control input, which mathematically doesn't affect the state variable under test. We see performance of our model does *not* change even under large perturbations.

Baseline			Baseline+SC			Ours-HD			Ours		
IID	OOD	(OOD-IID)/IID	IID	OOD	(OOD-IID)/IID	IID	OOD	(OOD-IID)/IID	IID	OOD	(OOD-IID)/IID
0.014	0.19	12.89	0.011	0.015	0.36	0.010	0.015	0.44	0.011	0.015	0.32

TABLE II: Results on electric motor dataset. Electric motor comes under the 4th scenario of our synthetic dataset.

prediction MSE for x_1 , and similarly, wiggling u_1^+ should not change the MSE for x_2 . An identical argument holds for scenario 2-3.

We present our results for four intervention experiments in Figure 5. MSE values have been reported for five-step predictions averaged across models trained with ten different random seeds. From the graphs 5a - 5d, we can conclude that our approach with factored representations along with separate decoders (**Ours**) is most likely to have captured the underlying relations perfectly. Having separate decoders guides learning such that each $\tilde{z}_{t+1}(i)$ specializes in that state's dynamics, hence inducing disentangled representations. The MSE for the baseline architecture blows up after we slowly increase the

standard deviation of the additive noise, indicating its poor ability to apprehend state-control interactions. For the model with separate control encoders and without factored representations (**Baseline+SC**), the MSE does not change much initially but increases gradually as the strength of intervention increases. In contrast, the error increases less gradually for the model with structural inductive bias (**Ours-HD**). The best performing models have a separable latent structure that is well matched to the data's nature. Our observations may also help explain why graph neural networks (GNNs), which treat each object as a separate node, are well suited for learning good object-centric representations [26], learning dynamic interactions [24] and discovering symbolic expressions [27].

B. Simulation: Electric Motor

Modeling electric motors is a challenging problem because of its very complicated dynamics. Prior work has been done on using a purely data-driven approach to model electric motors without making any assumptions on its internal behavior [23]. We intend to evaluate our models on their ability to capture complex dynamics that are part of everyday life and analyze how well they can generalize to unseen combinations of controls in this context. Hence, we test our framework to a dataset (80k data points) generated using a three-phase permanent magnet synchronous motor (PMSM) model available at GEM toolbox [22].

1) *Setup*: As described in [22], PMSM consists of three phases, where each voltage has an associated phase voltage and a phase current. A series of transformations convert these three-phase voltages and currents into d-q coordinates fixed to the rotor. Hence, our dataset consists of currents i_d, i_q , voltages u_d, u_q and rotor speed ω_r . As we are using segment-based modeling, we make sure that rotor speed, ω_r remains constant across that segment of length T . This leaves us with u_d, u_q acting as control variables and i_d, i_q acting as state variables. Other physical quantities associated with motor dynamics such as flux, inductance, and resistance are fixed.

Figure 6 shows the joint distribution of the controls (u_d, u_q) for PMSM dataset. To test a systematic generalization of our models, we make sure that they are only exposed to the first and third quadrant of the control's joint distribution (Marked with Blue in Figure 6). We make sure that the controls are sampled from the second and fourth quadrant only during out-of-distribution testing, enabling generalization testing to the unseen combination of (u_d, u_q).

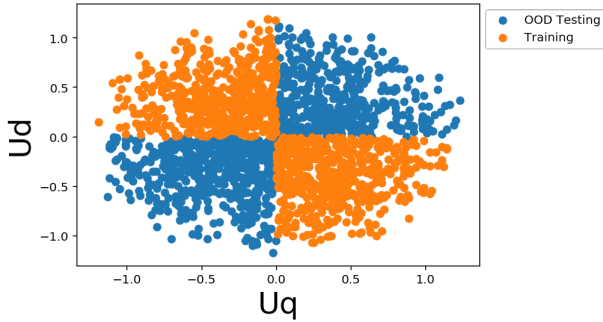


Fig. 6: Distribution of control inputs for electric motor dataset.

2) *Results*: We train our models on the simulated PMSM system (4k temporal segments; $T = 10$) using 5-step prediction over ten different random seed initializations. Testing is performed over 1k segments for this experiment. We evaluate if the latent transition models can capture real-world physical systems' complex internal dynamics and forecast up to large horizons while generalizing systematically.

a) *Forecasting – IID vs. OOD Performance*: We report the MSE values for the models' predictions five steps into the future in Table II. MSE values for IID data are reported on the simulated data's testing set. The baseline model performs

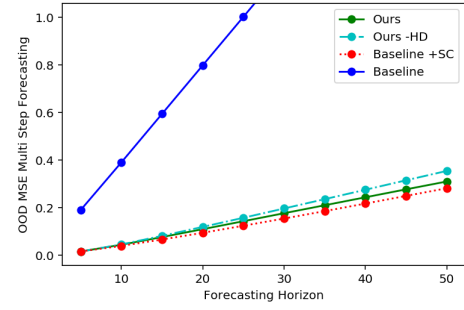


Fig. 7: Variation of OOD loss with forecasting horizons.

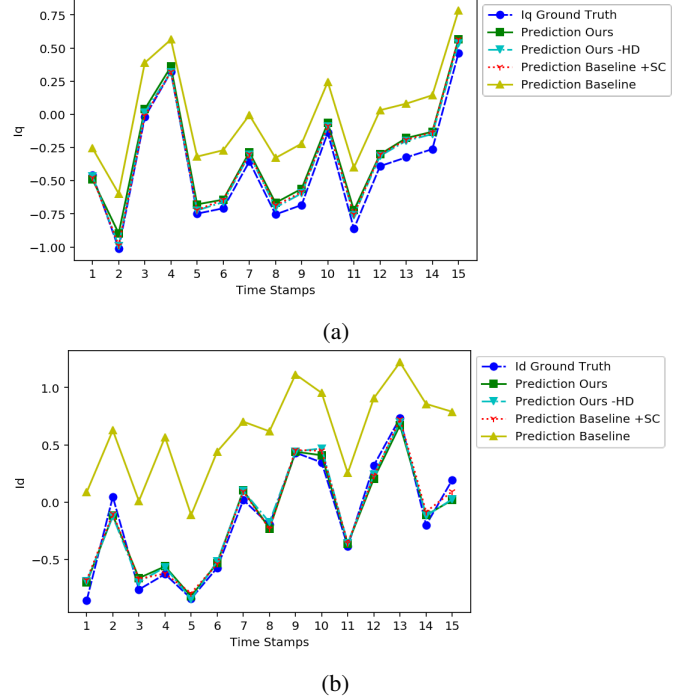


Fig. 8: Forecasting of i_q and i_d variable, when subjected to OOD control inputs, over a 15 time-stamp forecasting horizon.

worse across all evaluation metrics. The model with factored transition model fits best to the IID dataset and achieves the lowest MSE on OOD data. Besides, we repeatedly observe the usefulness of treating each factored representations while decoding as it performs the best (lowest). Thus, the models with better structural inductive bias can learn some form of systematic generalization and capture the complex internal dynamics as well.

b) *Forecasting up to large horizons*: It is evident to question the model's ability to forecast well up to horizons larger than those used to train them. We present Figure 7 and Figure 8 to understand the model's forward predictive abilities for large horizons, up to 50-time steps in the future given they have been trained with 5-step predictions.

Figure 7 shows the accumulated MSE on out-of-distribution dataset for the models in consideration. In corroboration with our previous quantitative results, we observe that the model

without any structured transition models suffers the most as the prediction horizon increases (**Baseline**). This indicates the poor quality of the learned transition model and possible overfitting to the training data. Besides, all the models with separate control encoding perform well on larger horizons (Architecture 2-4 in Figure 2), with the models having additional factored latent representations performing slightly better than its counterpart on horizons between 40-50.

To understand how closely do the architectures model the ground truth future state time series, we present Figure 8 consisting of the ground truth future state time series from the OOD dataset for the PMSM states i_d, i_q along with the predictions from all the models. Figure 8a shows that the baseline architecture can capture the ground truth trajectory's overall pattern with some bias, which increases with time. However, Figure 8b indicates that the baseline model does a poor job at capturing the trajectory of i_d perfectly, even for the first few forecasting steps. Providing additional prior in terms of the separate encoder for the controls helps capture the trajectories well.

VII. CONCLUSION

In this work, we conducted a rigorous study of systematic generalization in the forward prediction model for highly nonlinear dynamical systems over temporal segments of states and controls (actions). We restrict our analysis to a fully observable environment with deterministic transition dynamics. We investigate how well different architectural inductive biases generalize to unseen combinations of the actions and find that having factored representations for states and control helps. Our finding is in corroboration with [5] where they highlight the usefulness of having modularity in the network [16] for language understanding.

Our work also showcases the value that can be derived from controlled-synthetic experiments. Even though multiple architectures were generalizing well across different NARMA scenarios, careful intervention testing indicated that some architectures were capturing the underlying dependency less than the others. Throughout our study, we assumed that the number of state variables equals the number of control variables, which might not be the case in many cases. Hence, designing better architectures that incorporates structural transition model is a key future direction.

REFERENCES

- [1] Mishra, Nikhil, Pieter Abbeel, and Igor Mordatch. "Prediction and control with temporal segment models." In International Conference on Machine Learning, pp. 2459-2468. PMLR, 2017.
- [2] Franceschi, Jean-Yves, Aymeric Dieuleveut, and Martin Jaggi. "Unsupervised scalable representation learning for multivariate time series." arXiv preprint arXiv:1901.10738 (2019).
- [3] Oord, Aaron van den, Yazhe Li, and Oriol Vinyals. "Representation learning with contrastive predictive coding." arXiv preprint arXiv:1807.03748 (2018).
- [4] Lake, Brenden, and Marco Baroni. "Generalization without systematicity: On the compositional skills of sequence-to-sequence recurrent networks." In International Conference on Machine Learning, pp. 2873-2882. PMLR, 2018.
- [5] Bahdanau, Dzmitry, Shikhar Murty, Michael Noukhovitch, Thien Huu Nguyen, Harm de Vries, and Aaron Courville. "Systematic generalization: what is required and can it be learned?" arXiv preprint arXiv:1811.12889 (2018).
- [6] Ruis, Laura, Jacob Andreas, Marco Baroni, Diane Bouchacourt, and Brenden M. Lake. "A benchmark for systematic generalization in grounded language understanding." arXiv preprint arXiv:2003.05161 (2020).
- [7] Gontier, Nicolas, Koustuv Sinha, Siva Reddy, and Christopher Pal. "Measuring systematic generalization in neural proof generation with transformers." arXiv preprint arXiv:2009.14786 (2020).
- [8] De Gooijer, Jan G., and Rob J. Hyndman. "25 years of time series forecasting." International journal of forecasting 22, no. 3 (2006): 443-473.
- [9] Lai, Guokun, Wei-Cheng Chang, Yiming Yang, and Hanxiao Liu. "Modeling long-and short-term temporal patterns with deep neural networks." In The 41st International ACM SIGIR Conference on Research & Development in Information Retrieval, pp. 95-104. 2018.
- [10] Muralidhar, Nikhil, Sathappan Muthiah, and Naren Ramakrishnan. "DyAt Nets: Dynamic Attention Networks for State Forecasting in Cyber-Physical Systems." In IJCAI, pp. 3180-3186. 2019.
- [11] Krizhevsky, Alex, Ilya Sutskever, and Geoffrey E. Hinton. "Imagenet classification with deep convolutional neural networks." Advances in neural information processing systems 25 (2012): 1097-1105.
- [12] Malhotra, Pankaj, Vishnu TV, Lovekesh Vig, Puneet Agarwal, and Gautam Shroff. "TimeNet: Pre-trained deep recurrent neural network for time series classification." arXiv preprint arXiv:1706.08838 (2017).
- [13] Chen, Ting, Simon Kornblith, Mohammad Norouzi, and Geoffrey Hinton. "A simple framework for contrastive learning of visual representations." In International conference on machine learning, pp. 1597-1607. PMLR, 2020.
- [14] Mikolov, Tomas, Ilya Sutskever, Kai Chen, Greg Corrado, and Jeffrey Dean. "Distributed representations of words and phrases and their compositionality." arXiv preprint arXiv:1310.4546 (2013).
- [15] Yan, Wilson, Ashwin Vangipuram, Pieter Abbeel, and Lerrel Pinto. "Learning predictive representations for deformable objects using contrastive estimation." arXiv preprint arXiv:2003.05436 (2020).
- [16] Andreas, Jacob, Marcus Rohrbach, Trevor Darrell, and Dan Klein. "Neural module networks." In Proceedings of the IEEE conference on computer vision and pattern recognition, pp. 39-48. 2016.
- [17] Fodor, Jerry A., and Zenon W. Pylyshyn. "Connectionism and cognitive architecture: A critical analysis." Cognition 28, no. 1-2 (1988): 3-71.
- [18] Calvo, Paco, and John Symons, eds. The Architecture of Cognition: Rethinking Fodor and Pylyshyn's Systematicity Challenge. MIT Press, 2014.
- [19] Kingma, Diederik P., and Jimmy Ba. "Adam: A method for stochastic optimization." arXiv preprint arXiv:1412.6980 (2014).
- [20] Atiya, Amir F., and Alexander G. Parlos. "New results on recurrent network training: unifying the algorithms and accelerating convergence." IEEE transactions on neural networks 11, no. 3 (2000): 697-709.
- [21] J. R. Maat, A. Malali, and P. Protopapas, "TimeSynth: A Multipurpose Library for Synthetic Time Series in Python," 2017. [Online]. Available: <http://github.com/TimeSynth/TimeSynth>
- [22] Traue, Arne, Gerrit Book, Wilhelm Kirchgässner, and Oliver Wallscheid. "Toward a Reinforcement Learning Environment Toolbox for Intelligent Electric Motor Control." IEEE Transactions on Neural Networks and Learning Systems (2020).
- [23] Verma, Sagar, Nicolas Henwood, Marc Castella, Francois Malrait, and Jean-Christophe Pesquet. "Modeling electrical motor dynamics using encoder-decoder with recurrent skip connection." In Proceedings of the AAAI Conference on Artificial Intelligence, vol. 34, no. 02, pp. 1387-1394. 2020.
- [24] Kipf, Thomas, Ethan Fetaya, Kuan-Chieh Wang, Max Welling, and Richard Zemel. "Neural relational inference for interacting systems." In International Conference on Machine Learning, pp. 2688-2697. PMLR, 2018.
- [25] Pearl, Judea. Causality. Cambridge university press, 2009.
- [26] Kipf, Thomas, Elise van der Pol, and Max Welling. "Contrastive learning of structured world models." arXiv preprint arXiv:1911.12247 (2019).
- [27] Cranmer, Miles, Alvaro Sanchez-Gonzalez, Peter Battaglia, Rui Xu, Kyle Cranmer, David Spergel, and Shirley Ho. "Discovering symbolic models from deep learning with inductive biases." arXiv preprint arXiv:2006.11287 (2020).